AFRL-SR-AR-TR-09-0243

REPORT DOCUMENTATION PAGE

PLEASE DO NOT RETURN YOUR FORM TO THE ABOVE ORGANIZATION.

1. REPORT DATE *(DD-MM-YYYY)*	2. REPORT TYPE	3. DATES COVERED *(From - To)*
20-07-2009	Final	01 April 2005-30 Jun 2009

4. TITLE AND SUBTITLE
BIOLOGICALLY INSPIRED NANO-CONTACT MECHANICS

5a. CONTRACT NUMBER

5b. GRANT NUMBER
FA9550-05-1-0210

5c. PROGRAM ELEMENT NUMBER

6. AUTHOR(S)
Pradeep R. Guduru

5d. PROJECT NUMBER

5e. TASK NUMBER

5f. WORK UNIT NUMBER

7. PERFORMING ORGANIZATION NAME(S) AND ADDRESS(ES)
Brown University
Division of Engineering
182 Hope St, Providence, RI 02912

8. PERFORMING ORGANIZATION REPORT NUMBER

9. SPONSORING/MONITORING AGENCY NAME(S) AND ADDRESS(ES)
AFOSR
875 N. Randolph Street Ste 325
Arlington, VA 2203

10. SPONSOR/MONITOR'S ACRONYM(S)

11. SPONSOR/MONITOR'S REPORT NUMBER(S)

12. DISTRIBUTION/AVAILABILITY STATEMENT
Distribution A: Unlimited

13. SUPPLEMENTARY NOTES

14. ABSTRACT
The objective of this project was to investigate the mechanics aspects of biological adhesion and friction mechanisms of small animals and insects and to extract canonical principles that can help design synthetic surface micro-architectures that can mimic the exceptional adhesion capabilities of these animals. Our approach included theoretical modeling, experimental validation of the models and fabrication & testing of microstructures. Significant progress has been made in developing a fundamental mechanistic understanding of adhesion and friction of soft and fibrillar surfaces, which motivates several novel bio-inspired designs for future development.

15. SUBJECT TERMS

16. SECURITY CLASSIFICATION OF:			17. LIMITATION OF ABSTRACT	18. NUMBER OF PAGES	19a. NAME OF RESPONSIBLE PERSON
a. REPORT	b. ABSTRACT	c. THIS PAGE			DR. PRADEEP GUDURU
U	U	U	U	26	19b. TELEPHONE NUMBER *(Include area code)* 401 863 3362

Final Report 2009

BIOLOGICALLY INSPIRED NANO-CONTACT MECHANICS

AFOSR Grant # FA9550-05-1-0210

Principal Investigator

Pradeep R. Guduru

Brown University
Division of Engineering
182 Hope St, Providence, RI 02912
Tel: 401 863 3362; Pradeep_Guduru@Brown.edu

Supported by

Air Force Office of Scientific Research
Mechanics of Multifunctional Materials & Microsystems
Program Manager: Dr. Les Lee

Summary

The objeetive of this project was to investigate the mechanies aspeets of biologieal adhesion and frietion meehanisms of small animals and inseets and to extraet eanonieal principles that ean help design synthetie surfaee miero-arehitectures that ean mimie the exceptional adhesion capabilities of these animals. Our approaeh ineluded theoretical modeling, experimental validation of the models and fabrieation & testing of mierostructures. Significant progress has been made in developing a fundamental mechanistie understanding of adhesion and friction of soft and fibrillar surfaces, whieh motivates several novel bio-inspired designs for future development. The highlights of the researeh outeomes are:

(i) Mechanies of wavy surfaee adhesion and frietion: We developed a theory to deseribe the contact instabilities at the surfaee of a rough surfaee whieh dissipate energy and lead to enhaneed adhesive strength and toughness. A detailed experimental study was earried out, whieh validated the predietions of the theory. For some of the experimental geometries eonsidered, surfaee waviness eaused the adhesion strength to inerease by a faetor of 17 eompared to the no-waviness case.

(ii) Direetion dependent adhesion strength through elastie anisotropy: We developed a theory of adhesion for anisotropie materials, whieh showed that an elastie adhesive surfaee ean show adhesion strength whieh depends on the direetion of detaehment. This result suggests a novel design principle for designing bio-inspired adhesive surfaces which can display strong and easy detaehment at the same time, simply by ehanging the foree direction.

(iii) Effect of eontaet shape on adhesion strength, theory and experiments: We developed a theory for adhesion of arbitrary axisymmetrie shapes and earried out experiments to validate the theory. These results highlight the need to optimize eontaet shape in order to maximize the adhesion strength of a fiber.

(iv) Theory and experiments on adhesion in the presenee of substrate streteh – a reversible adhesion strategy: We developed a theoretical model to calculate the contact area as a function of substrate streteh and the assoeiated detaehment instabilities. An assoeiated experimental study validated the theoretical model, whieh also provided a eonvenient way to measure the work of adhesion as a function of mode mixity.

(v) Fabrieation of surfaee miero-arehiteetures that exhibit direetion dependent detachment strength and friction: A microfabrication technique was developed to make microstructures which show mueh higher adhesion strength eompared to a bulk surfaee.

The above results have appeared in several publieations and eonferenee presentations. The PI has been invited to present the above work at several peer institutions. The PI also organized symposia and workshops on bio-inspired struetural and materials design. The grant supported the work of a graduate student, two postdoes (partial) and several undergraduate researeh assistants. These details are listed at the end of this report.

Biologically Inspired Nano-Contact Mechanics

Background

The ability of small animals such as insects, flies and geckos to climb up vertical walls and to walk up side down on ceilings has been a subject of active research in biology for many centuries. There is a variety of mechanisms employed by these animals, including tiny claws, adhesive secretions, smooth and hairy adhesive pads, etc. Following the accumulation of a large body of anatomical and functional data on various natural adhesion systems, in the last few years biologists and engineers have been working together to develop a quantitative understanding of various natural adhesion and friction systems. This is a growing field of research with a rich set of challenging problems at the interface between biology, applied mechanics and micro/nano-fabrication, with potentially significant benefits if we can understand and mimic some of nature's optimized solutions for technological advancement. Moreover, an attempt to develop quantitative understanding of the biological attachment systems and synthetic biomimetic systems leads to several basic problems in the mechanics of adhesive contact and sliding. Thus findings in this area will be of interest to a broader range of researchers. Our approach consisted of identifying a series of sub-projects of broader interest and investigate them analytically and experimentally. The work reported below has appeared in peer-reviewed journal articles and conference proceedings.

(1) Theory and Experiments on the Mechanics of Wavy Surface Adhesion

The basic question here is to understand the role of surface roughness or waviness in adhesion strength of an insect foot with smooth foot pads. We developed a theory of wavy surface adhesion, in which the mechanics of detachment of a rigid solid from an elastic wavy surface has been analyzed for the axisymmetric case of a sphere and the plane strain case of a cylinder, as shown in Fig. 1a. The solution procedure consists of solving the contact problem by means of the cumulative superposition method and correcting it for the presence of adhesion. The details of the solution procedure can be found in Guduru [2007]. A representative solution for the load-displacement curve for a sphere indenting a wavy flat surface is shown in Fig. 1b, in which the load P is normalized with the JKR pull-off force P_{JKR} and the approach displacement h is normalized with the waviness amplitude λ.

It is shown that the surface waviness makes the detachment process proceed in alternating stable and unstable segments and each unstable jump dissipates mechanical energy, as illustrated in Fig. 2a. As a result, the external work and the peak force required to separate a wavy interface are higher than the corresponding values for a flat interface; i.e., waviness causes interface toughening as well as strengthening. Thus, contrary to conventional thinking, surface waviness can make soft surfaces adhere better by introducing mechanisms of energy dissipation. This is the main finding of this analysis, with important consequences not just for insect adhesion problems, but also for a wide variety engineering problems of interest such as rubber adhesion.

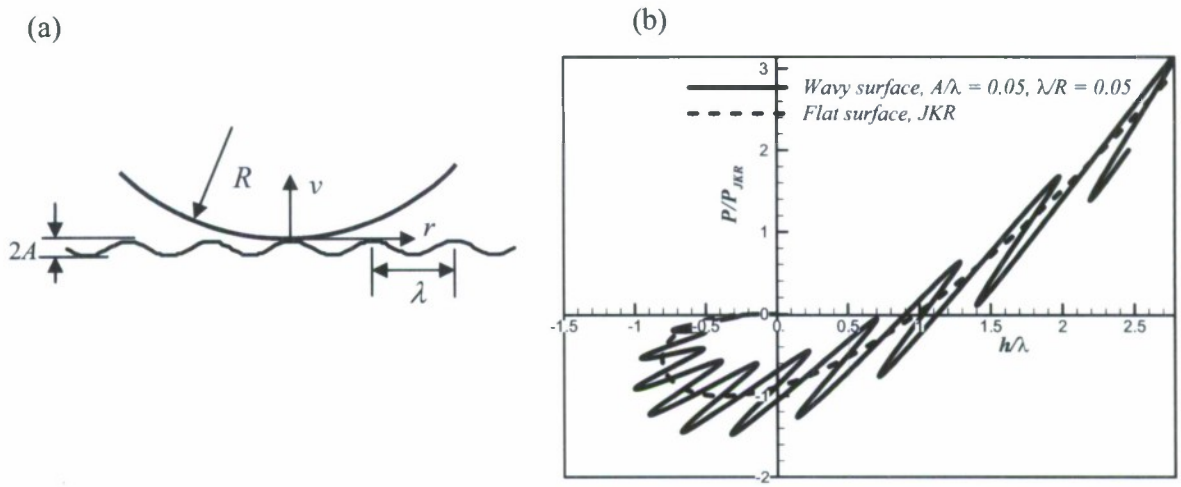

Fig.1 (a) The geometry of the problem. A sphere (or cylinder) of radius R contacts an elastic half space with a single wavelength cosine surface. (b) The force-deflection curve for wavy surface adhesion (solid curve), superposed on top of the classical JKR curve (dashed). The presence of waviness modifies the JKR result such that there is an increase in pull-off force due to the oscillations of the force-deflection curve.

A systematic experimental investigation has been carried out which examines predictions of the above theoretical analysis, by measuring adhesion between a "rigid" wavy punch and a soft "elastic" material. Gelatin has been chosen as the model soft material in our experiments. The observed increase in adhesion due to waviness closely agrees with the theoretical predictions (within the experimental and material uncertainties), as shown in Fig. 2b. Note that the increase in the adhesion strength is non-trivial. For example, for the experimental parameters, waviness causes the attachment strength to increase by a factor of about 15, by simply modifying the surface topography! The experiments not only validate the theory, but also demonstrate that adhesion of a soft material can be substantially enhanced by topographic optimization alone, without modifying the surface chemistry. Complete details of the experimental procedures and results can be found in Guduru and Bull [2007].

A sequence of papers describing this work appeared in the Journal of the Mechanics and Physics of Solids and the International Journal of Solids and Structures.

(i) P.R. Guduru. Detachment of a rigid solid from an elastic wavy surface: Theory. *Journal of the Mechanics and Physics of Solids*. 55 (2007), 445–472.

(ii) P.R. Guduru and C. Bull. Detachment of a rigid solid from an elastic wavy surface: Experiments. *Journal of the Mechanics and Physics of Solids*. 55 (2007), 473–488.

(iii) J.F. Waters, S. Lee, P.R. Guduru. Mechanics of axisymmetric wavy surface adhesion: JKR-DMT transition solution. Accepted for publication in *International Journal of Solids and Structures*, 2008.

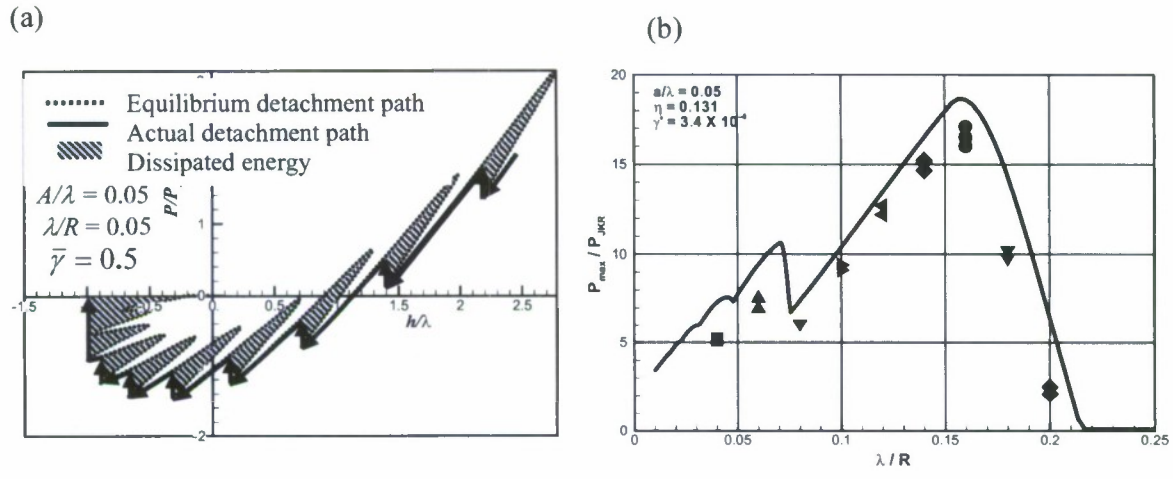

Fig 2. (a) Energy dissipation due to unstable detachment of a sphere from an axisymmetric wavy surface. Dashed curve is the equilibrium path and the solid line is the actual path followed in displacement controlled loading. Each vertical solid line segment represents an unstable jump during which the crack advances spontaneously to the next available stable position. The hatched area adjoining each unstable segment is the mechanical energy dissipated during that crack jump. (b) Summary of experimental data on adhesion force as a function of wavelength: comparison between the experimental measurements (symbols) and theoretical predictions (solid lines). Experimental results capture not only the magnitude of the predictions, but also features such as the local maxima.

(2) Orientation-dependent adhesion strength due to elastic anisotropy

It has been revealed that the extraordinary ability of geckos to climb on vertical walls and ceilings essentially stems from the van der Waals force (Autumn et al., 2000). To take advantage of the extremely weak intermolecular forces, geckos have developed hundreds of thousands of tiny fibers on their feet. Each fiber, referred to as seta, is split further into hundreds of thinner branches called spatulae. Such hierarchical fibrillar structures have apparently allowed gecko to achieve robust adhesion with solid surfaces irrespective of surface roughness (Arzt et al., 2003; Gao and Yao, 2004). More interestingly, the adhesion force of a single seta was found to be strongly dependent on the pulling direction. Strongest adhesion was measured at a pulling angle of around 30° with respect to the surface (Autumn et al., 2000). Such directional adhesion force can be partly attributed to the asymmetrical geometry of a single seta (Gao et al., 2005). On the other hand, the direction-dependent adhesion strength also turns out to be a generic phenomenon associated with anisotropic elastic solids, as shown by Yao and Gao (2006) for a cracked interface between an anisotropic material and a rigid substrate. Chen and Gao (2007) made the first attempt to develop a real contact model for this phenomenon by considering a rigid cylinder in contact with a transversely isotropic elastic solid subjected to an inclined pulling force. However, an implicit assumption made in the study of Chen and Gao (2007) was that the contact

region remains symmetric with respect to the center of the cylinder. It was not realized until recently that this assumption was not self-consistent because the resulting energy release rates at the two contact edges differed from each other. We revisit the problem adhesion between a cylinder and a transversely isotropic elastic half space and derived the correct solution without an assumption on the symmetry of the contact region.

Figure 3 shows the geometry of the problem being analyzed. Note that the x_0 and y_0 axes are aligned with the minimum and maximum directions of the elastic modulus of the half space. The rigid cylinder is in contact with the half space over a contact region of width $(a+b)$ and a detachment force F is applied at an angle ϕ. The task here is to solve for the critical detachment force F as a function of the detachment angle ϕ, when the anisotropy ratio (the ratio of the maximum modulus to the minimum modulus) is varied. The details of the solution procedure can be found in Yao et al. [2008]. Here only a representative result is presented in Fig. 4, which shows the detachment force F as a function of the detachment angle. It shows the results for four different values of θ, i.e. the orientation of the elastic anisotropy axes with respect to the top surface, as illustrated in Fig. 3. The primary conclusion of this analysis is that elastic anisotropy causes the adhesion strength to be direction dependent. Thus, this is a powerful design principle in new materials to achieve anisotropic adhesion strength, which will have directions of strong attachment and directions of easy detachment. This work has been accepted for publication in the following article.

(i) H. Yao, S. Chen, P.R. Guduru, H. Gao. Orientation-dependent adhesion strength of a rigid cylinder in non-slipping contact with a transversely isotropic half-space. Accepted in *International Journal of Solids and Structures*, 2008.

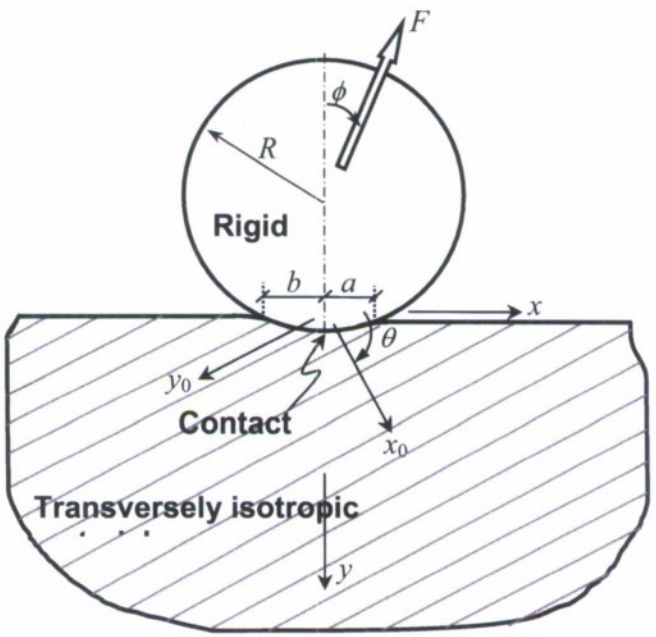

Figure 3. A rigid cylinder of radius R in non-slipping contact with a transversely isotropic elastic half-space with its symmetry axis inclined at angle θ with respect to the normal of the surface. Cartesian coordinate systems (x_0, y_0) and (x, y) refer to the material coordinates and fixed coordinates, respectively. An external pulling force F is applied on the cylinder at an angle ϕ with respect to the y-axis.

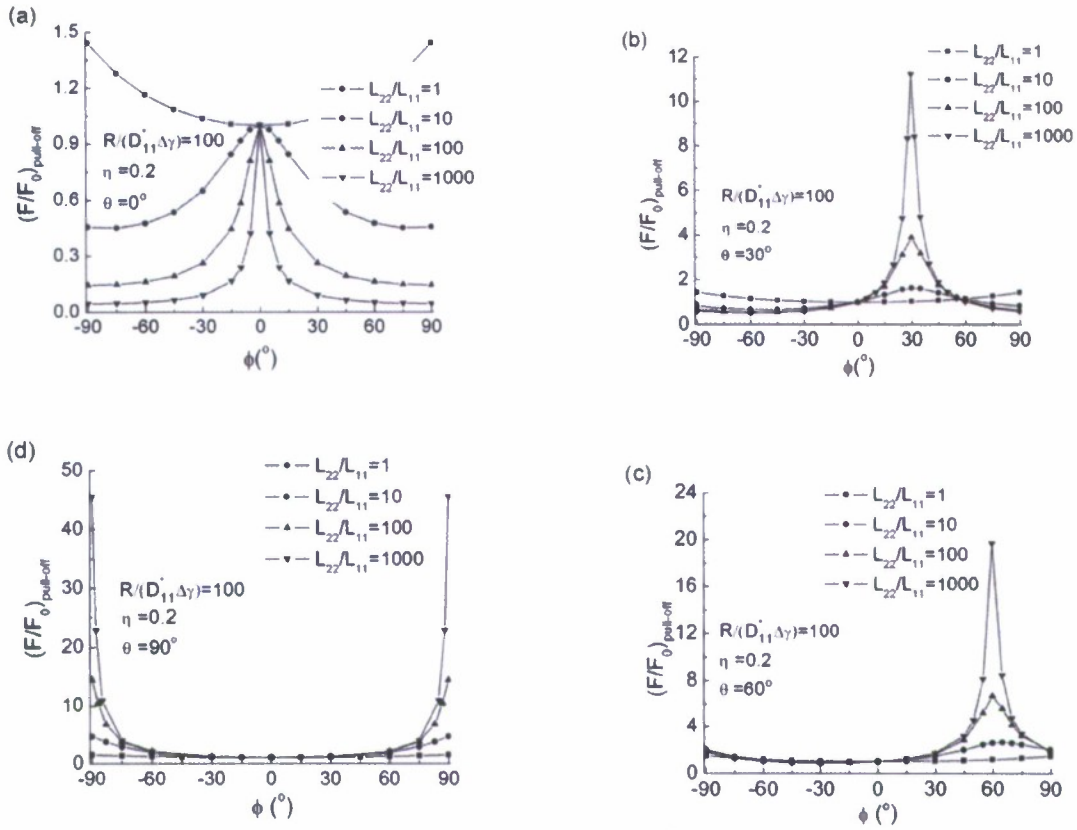

Figure 4. The normalized pull-off force $(F/F_0)_{\text{pull-off}}$ as a function of the pulling angle ϕ for $\eta = 0.2$, $R/(D_{11}^{*}\Delta\gamma) = 100$, $L_{22}/L_{11} = 1$, 10, 100, 1000 with tilting angle θ equal to (a) 0°, (b) 30°, (c) 60°, (d) 90°, respectively.

(3) Maximum strength for intermolecular adhesion of nanospheres at an optimal size

Intermolecular forces, although usually much weaker than interatomic forces, are known to play important roles in many physical properties such as melting point, vapor pressure, evaporation, viscosity and surface tension. Recent studies have shown that intermolecular forces also play a dominant role in the reversible adhesion mechanisms of gecko and many insects (Autumn et al., 2000, 2002; Arzt et al., 2003). The bottom surfaces of the toes of gecko are covered with scale-like structures called lamellae; each lamella is coated with hundreds of thousands of fibers called setae; each seta is about 110 μm long and further branches into hundreds of 200–500 nm nano-hairs called spatulae. This hairy structure of gecko represents a class of convergent evolution for dry adhesion. Among hundreds of animal species that have adopted similar hairy adhesion structures, gecko stands out in terms of its body weight and its extraordinary ability to maneuver on vertical walls and ceilings. Arzt et al. (2003) discussed an

interesting correlation between the size of the smallest hairs of animals and their body weight: the heavier the animal, the smaller the hairs, and gecko's spatulae are the smallest. This size effect has stimulated a number of theoretical studies showing that the adhesion strength between solid objects generally tends to increases as the characteristic size of the objects is reduced and eventually saturates at the theoretical adhesion strength below a critical size (Persson, 2003; Gao & Yao, 2004; Tang et al., 2005; Gao et al., 2005).

A common view shared by most of the existing studies is that the strength of intermolecular adhesion is a non-decreasing function of the size of the contacting objects. However, these studies have all made an implicit assumption that intermolecular adhesion can be described as interaction between two adjacent surfaces. In this study, we show that this assumption is not valid if one of the contacting objects is a nano-particle, in which case intermolecular adhesion can no longer be described as an interaction between two solid surfaces because the particle itself may become completely immersed in the interaction zone. In fact, we show that intermolecular adhesion between two spheres or between a sphere and a solid half-space exhibits a peak value at an optimal size determined by a transition between surface dominated and bulk dominated interaction regimes at nanoscale.

Intermolecular forces can be either attractive or repulsive. The most dominant attractive force is the van der Waals force which has an interaction energy inversely proportional to the sixth power of the intermolecular separation r, i.e. $U_a(r) \propto r^{-6}$. In comparison to the attractive force, the repulsive force has a much shorter interaction range. A common description of the repulsive force is $U_r(r) \propto r^{-n}$, where n is an integer normally between 9 and 16. A common interaction potential between two molecules is the 6-12 *Lennard-Jones* (LJ) potential,

$$U_{\mathrm{LJ}}(r) = A/r^{12} - B/r^{6}$$

where A and B are constants.

Assuming intermolecular potential is additive, the interaction potential between two solid objects can be obtained by integrating the LJ potential over the material domains. Calculations of this type were first made by de Boer (1936) and Hamaker (1937) (e.g. Israelachvili, 1992). For example, the interaction potential between a single isolated molecule at a distance D from a solid half-space is obtained by summing up the interactions between the isolated molecule and all molecules in the solid as

$$U(D) = 2\pi\rho_1 \int_D^\infty \mathrm{d}z \int_0^\infty \left[\frac{A}{\left(z^2 + x^2\right)^6} - \frac{B}{\left(z^2 + x^2\right)^3} \right] x\mathrm{d}x = \pi\rho_1 \left(\frac{A}{45D^9} - \frac{B}{6D^3} \right).$$

Now, consider the interaction force between a sphere and a half space as shown in Fig. 5a. The details of the calculations are given in Yao et al. [2008], by which the maximum adhesion force can be determined as a function of the sphere size. Figure 5*b* plots the calculated pull-off force $F^c_{\mathrm{S-}SS}$ as a function of the radius R of the sphere. One can see that for small spheres, $F^c_{\mathrm{S-SS}}$ is proportional to R^3, suggesting that the pull-off force is dominated by the volume of the sphere. As the sphere grows, such cubic dependence evolves asymptotically into a linear dependence, signifying a transition between the bulk dominated regime at very small sizes to the surface dominated regime at large sizes. Figure 5*c* shows the evolution of $F^c_{\mathrm{S-}SS} / \pi w_{ad} R$ with R/z_0. As $R \to \infty$, it is seen that the pull-off force asymptotically approaches the prediction

$F^c_{S-SS} / \pi w_{ad} R \to 2$ from classical Bradley and DMT models (Bradley, 1932; Derjaguin et al., 1975).

Figure 5*d* shows the normalized adhesion strength $F^c_{S-SS} / \pi R^2$ as a function of the radius of the sphere. For $R >> z_0$, the adhesion strength rises as R decreases and reaches a peak value of $0.65\sigma_{th}$ at $R \approx z_0$. Other than the coefficient 0.65, this peak value agrees with the prediction of the inter-surface force model. However, as R decreases further, instead of saturating at a limiting value as would be predicted by the inter-surface model, the adhesion strength actually drops down to zero. Such a behavior is due to the R^3-dependence of the pull-off force at small size scale and can not be captured by inter-surface force models. The behavior shown in Figure 5*b* that the pull-off force changes from a linear (R) dependence to a cubic (R^3) dependence as R decreases holds also for contact between two elastic solids. Similar conclusions can be drawn for other geometries such as interaction between two spheres and a cylinder and a half space.

The main result of this work is, we have shown that the conventional inter-surface force models fail to describe correctly the interaction force between two spheres at the small size limit. This is demonstrated by directly integrating the intermolecular forces between two spheres to examine the size dependence of adhesion strength at small scales. Our analysis is thus more rigorous than the inter-surface force models in adhesive contact mechanics. Our results showed that the adhesion strength between two spheres or between a sphere and a solid half-space exhibits a peak value at an optimal size, and eventually drops to zero as the size decreases further. We also showed that the adhesion strength between a hemisphere-ended cylinder and a solid half-space would saturate at the theoretical adhesion strength below a critical size in agreement with predictions from inter-surface force models. Therefore, it can not be generally concluded that the adhesion strength would (or would not) saturate at small contact size. Whether such saturation actually occurs depends on the limit of interaction volume at small sizes. If the interaction volume scales with the characteristic size R of the system as R^3, as in the case of nano-particles, there will be no strength saturation but a maximum strength at an optimal size. If the interaction volume scales as R^2, as in the case of hairs/fibers, the adhesion strength will eventually saturate at the theoretical adhesion strength. Although the present study has been based on the assumption of rigid solids, we expect that the conclusion should hold at least qualitatively for contact between elastic solids.

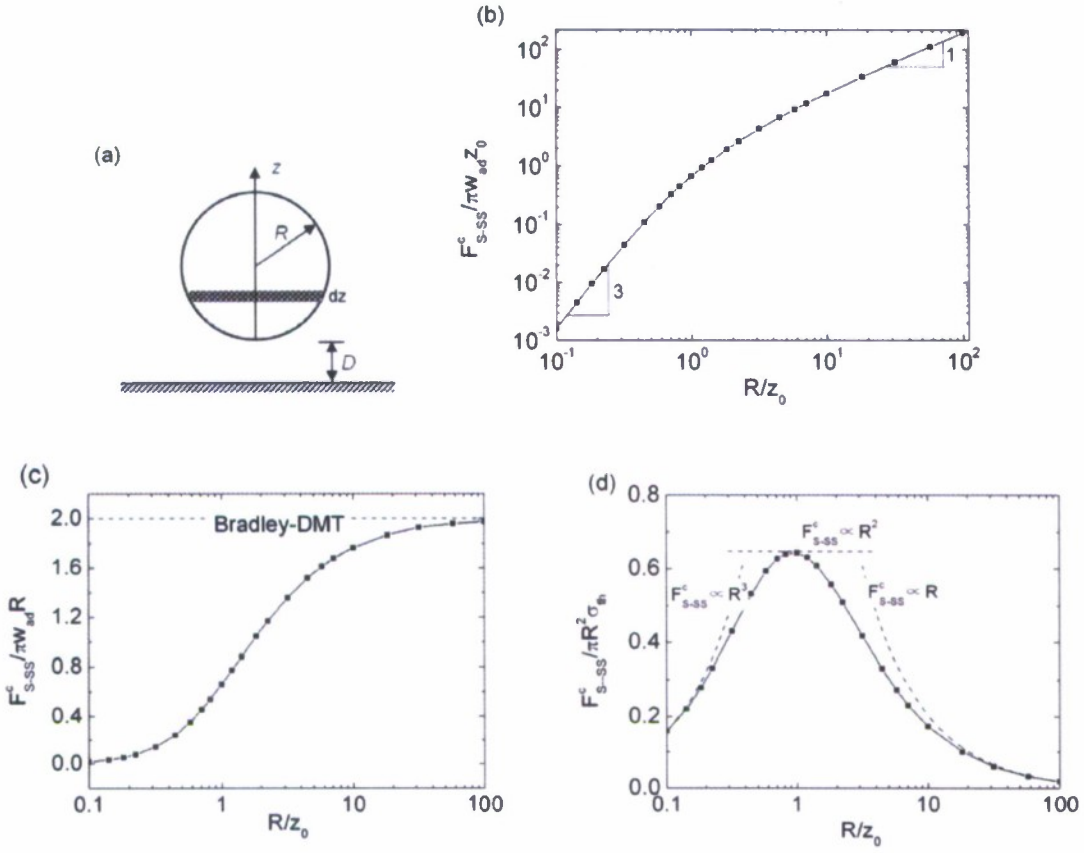

Figure 5. (a) Schematic illustration of a sphere (S) in adhesive contact with a solid half-space (SS). Scale dependence of the pull-off force normalized by (b) $\pi w_{ad} z_0$ and (c) $\pi w_{ad} R$; (d) Scale dependence of the normalized adhesion strength.

(4) Adhesion and Sliding Response of a Biologically Inspired Fibrillar Surface:

Recent work (Autumn *et al.* 2000) has demonstrated that the micro and nano-scale architectures of the gecko foot fibers are responsible for the animal's excellent attachment capability; this work has led to several investigations describing the mechanics of insect attachment as well as creating surface engineering strategies to mimic it. A key feature of gecko and other insect attachment is the ability to quickly switch between strong adhesion and easy detachment, which is essential in locomotion. Thus, any synthetic surface architecture needs to demonstrate the dual requirements that it should have strong adhesion and at the same time, the ability to quickly switch between the states of strong adhesion and easy detachment.

In order to realize these requirements, we developed a "*film terminated tilted fiber array*" architecture and we demonstrated its behavior in a system made of PDMS. The main observations of this effort are as follows. (i) The pull-off force increases with fiber tilt angle. (ii) There exists a direction of minimum pull-off force, which tends to become sharp with increase in fiber tilt angle. (iii) Under constant tensile normal force, fibrillar surfaces show highly

anisotropic sliding resistance. The film terminated tilted fibrillar sample is shown schematically in Fig. 6(a) and an image of which is shown in Fig. 6(d). In order to carry out adhesion and friction experiments, we designed and built a microtribometer, which is shown in Fig. 6(b), (c) & (e). Adhesion and friction experiments were carried out by bringing a spherical glass lens into contact with the sample. In order to assess the adhesion and friction behavior of the tilted fiber samples, two types of experiments were carried out, (i) directional adhesion experiments and (ii) sliding under negative load, which are described below.

(i) Directional adhesion experiments: In these experiments, the spherical probe is brought into contact with the sample and is retracted at angles spanning between -90° and 90° (0° corresponds to normal retraction). The main conclusion from these experiments, as summarized in Fig. 7, is that the fiber tilt angle of 40° results in increase in adhesion by a factor of 3 compared to bulk PDMS. Within the range of angles considered, the detachment force increases with increasing tilt angle. This is an extremely promising result because we observed the increase by a factor of 3 without any optimization of the geometry of the surface architecture. With careful selection of the fiber diameter, aspect ratio, sparing, film thickness and angle, it should be possible to realize much greater increase in adhesion. However, in order to carry out such an optimization, it is necessary to develop analytical models of how these parameters affect the detachment force. We are currently developing such models, which will be used to develop more refined architectures in near future.

(ii) Sliding under tensile force: In these experiments, the combined adhesion-friction behavior is characterized by measuring the critical tangential force necessary to cause separation or sliding under a constant normal tensile force. A constant normal tensile force is applied between the sample and the probe sphere while the sample is translated laterally at a constant velocity. The main results of these experiments are described in Figs. 8 and 9. Under constant tensile normal load, the vertical fiber samples display a fascinating switch from easy pull-off to very strong sliding resistance with a small perturbation in the normal load, similar to a phase transformation. This situation is very different from the response of bulk samples, which show an almost linear relation between the normal load and the critical tangential force. Moreover, the response of tilted fiber samples under sliding has two branches. In the positive direction along the tilt, they behave similar to the vertical fiber samples, showing the sudden transition from pull-off to no-separation. In the negative direction, the response is similar to that of the bulk samples. Thus, the tilted fiber samples display a strong anisotropy in sliding resistance. It is necessary to develop a quantitative description of the above observations to optimize the desired behavior and to develop the considered surface architecture for practical applications.

Thus, the tilted fiber geometry is a promising bio-architecture for anisotropic adhesion surfaces, which show a very rich behavior. Mathematical models to capture the essential features of the observed behavior are currently being developed and will be pursued further. The work described above has appeared in the following publication.

H. Yao, G. Della Rocca, P.R. Guduru and H. Gao. Adhesion and Sliding Response of a Biologically Inspired Fibrillar Surface: Experimental Observations. *Journal of the Royal Society Interface*. DOI: 10.1098/rsif.2007.1225. 2007.

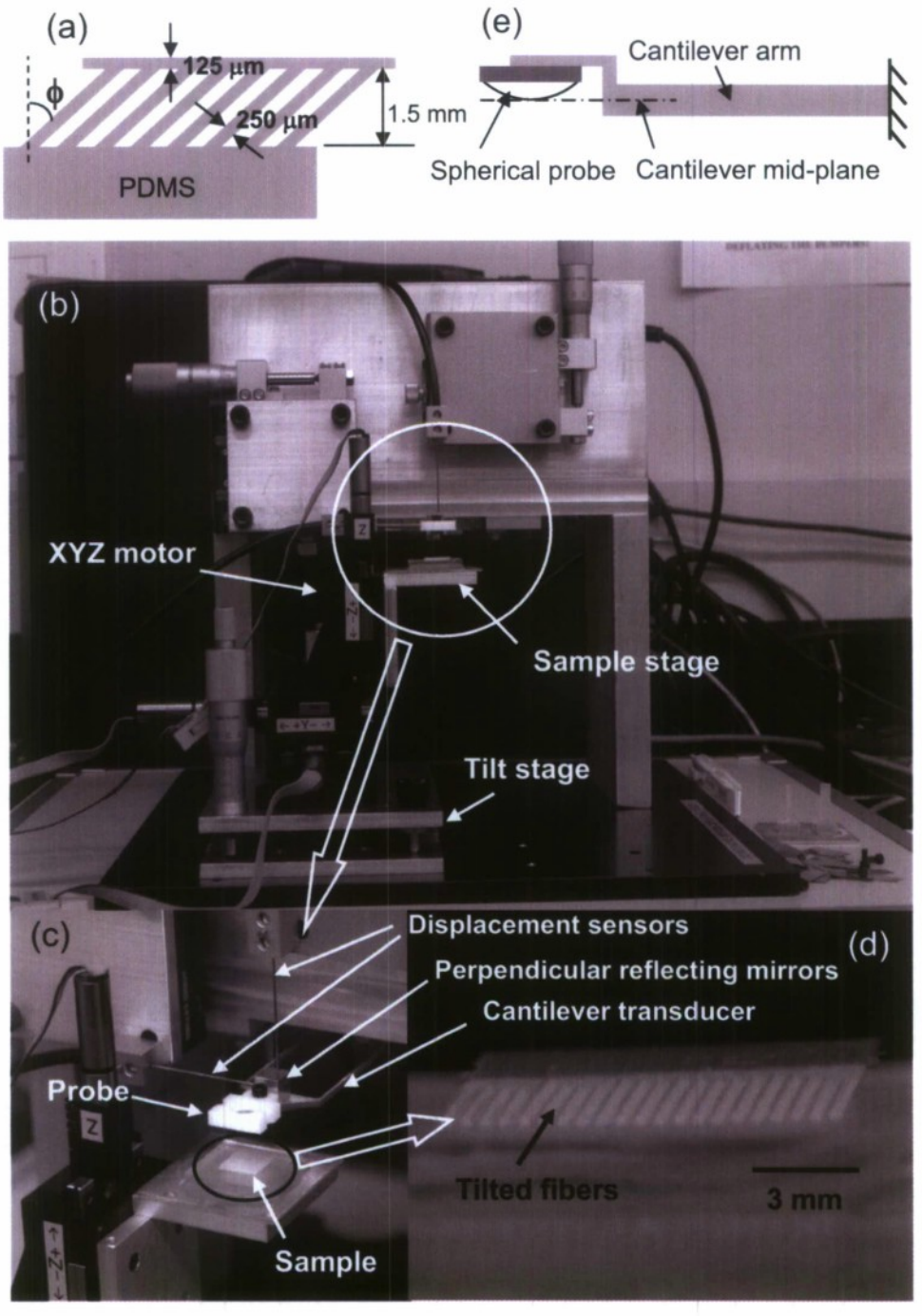

Figure 6. (a) Schematic illustration of the geometry of the film terminated tilted fiber samples. (b) A photograph of the setup to measure normal and lateral forces during directional adhesion and sliding experiments. (c) A detailed view of the sample, probe, cantilever and displacement sensors. (d) A photograph of the film terminated tilted fiber sample. (e) Schematic illustration of the cantilever and spherical probe assembly, in which the bottom plane of the probe coincides with the mid-plane of the cantilever in order to minimize cross-talk between the normal and the lateral force measurements.

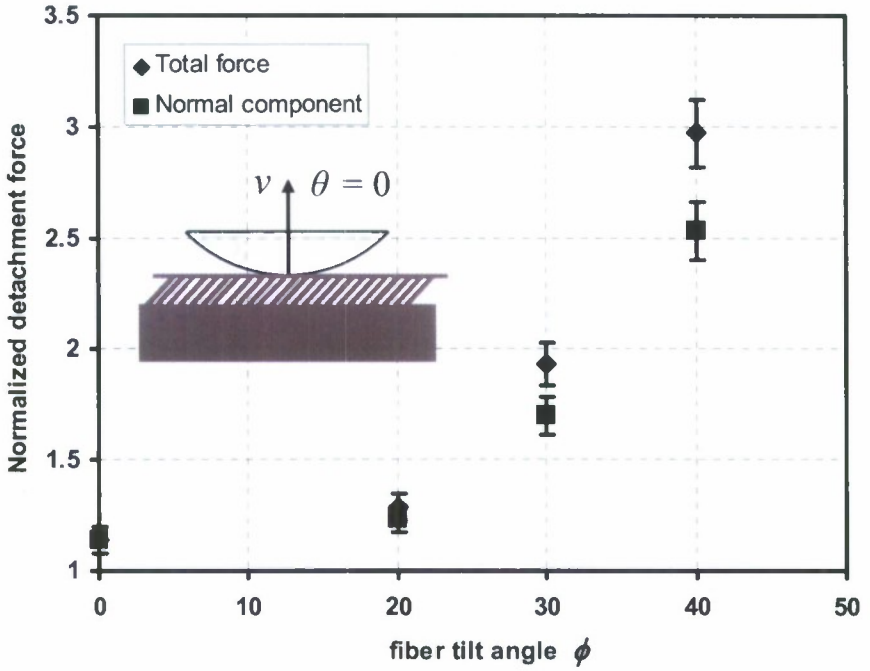

Figure 7. Normalized detachment force along $\theta = 0^{\circ}$, as a function of the fiber tilt angle ϕ. The detachment force is normalized with the normal pull-off force for bulk PDMS. The plot shows the total detachment force as well as its normal component.

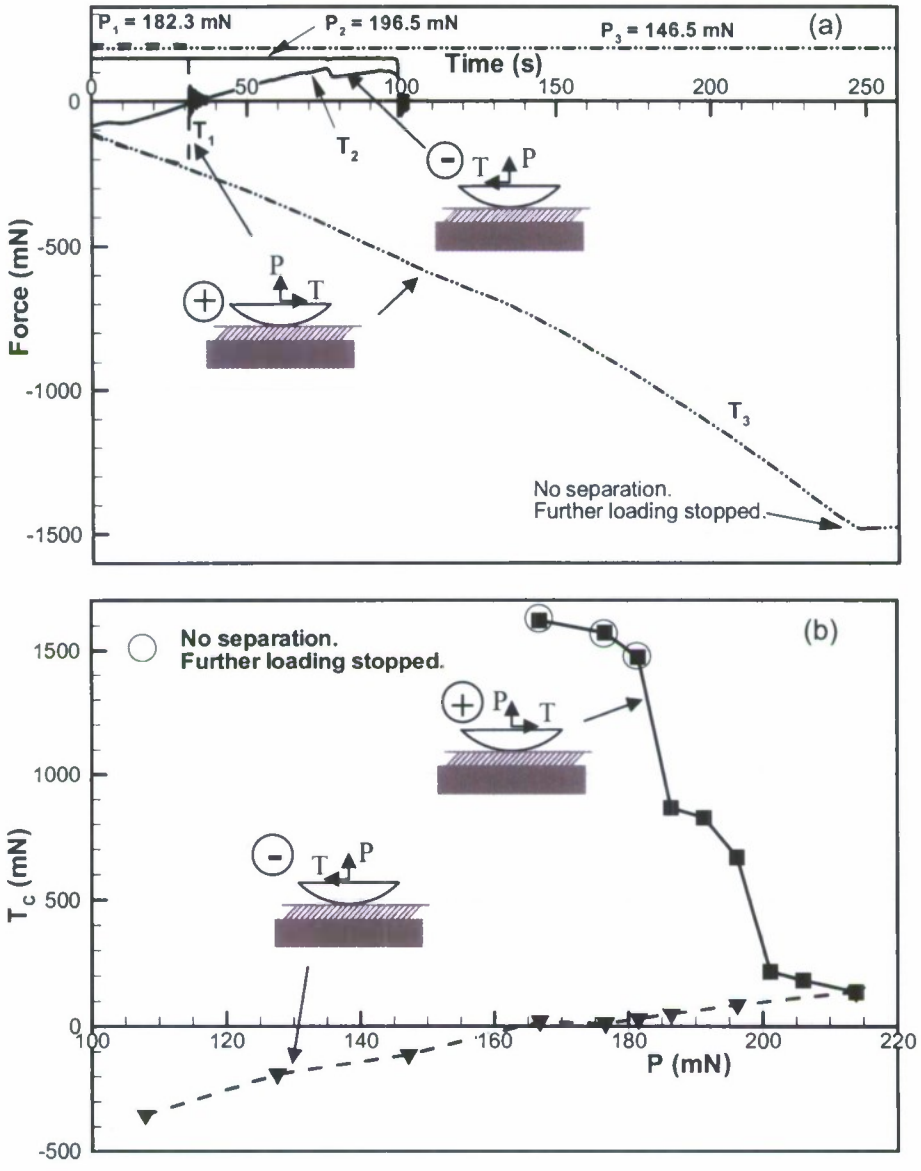

Figure 8. Sliding under tensile force – results for tilted fiber samples ($\phi = 40^{\circ}$). (a) History of normal (P) and tangential (T) forces during sliding. For sliding in positive direction, the behavior is similar to the vertical fiber samples, i.e., sliding resistance undergoes an almost step change with the normal force P. (b) Critical tangential force T_c as a function of normal tensile force P. The response in the negative direction (against the fiber tilt) is similar to that of the bulk PDMS, i.e., T_c increases almost linearly with decrease in P. The estimated measurement error is approximately ±5%.

(5) Optimal shapes for adhesion

Observations of the shapes of the fiber tips in several insect species revealed that they possess slight concavity, as illustrated in Fig. 9. Such observations have led to an investigation of optimal shapes for adhesion. By assuming that the interface fails when a critical normal stress is reached, Gao et al. (2006) derived an optimal concave shape to maximize the detachment force. In this work, we developed general solution for the detachment of any axisymmetric concave punch, within the assumptions of the linear elastic fracture mechanics. Further, we also showed that the solution of Gao et al. (2006) can be obtained as a special case of our generalized treatment of concave indenters. To illustrate the solution, consider the case of a spherically concave rigid indenter shown in Fig. 10, which illustrates a rigid cylindrical punch, indenting an elastic half space. The punch is a spherically concave at its bottom and the depth of the concavity is u_2, d is the depth of indentation, b is the radius of punch and P is the applied force. In the presence of adhesion, a negative force P is necessary to separate the two solids. It can be shown that the stress intensity factor at the contact edge is given by

$$K_I = \frac{E^* d}{\sqrt{\pi b}}\left(1+\frac{u_2}{d}\right)$$

and the pull-off force can be shown to be

$$P_{pull-off} = \sqrt{8\pi E^* b^3 \gamma} + \frac{8}{3} E^* b u_2$$

In the above expression, note that the first term on the right hand side is the pull-off force for a flat cylinder and the second term is the addition due to concavity. Note that for all positive values of u_2, i.e., concave shapes, the pull off force increases! The details of the above solution procedure are currently being prepared for publication.

We also carried out a parallel experimental investigation to validate the above analytical predictions and very good agreement was seen between the experiments and the theory, as illustrated in Fig. 11. Again, full details of these experiments will appear in an upcoming publication.

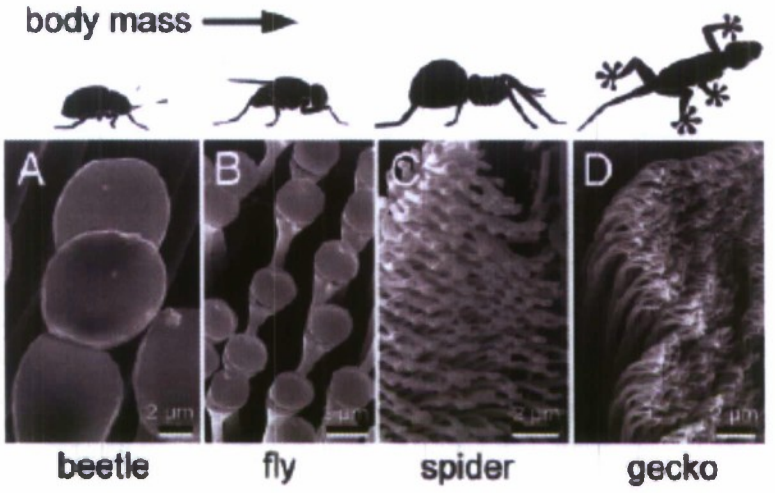

Figure 9. Microscopic images of the fiber tips on the feet of beetles and other animals. Notice the slight concavity of the tips for beetles. Figure is taken from: H. Gao & H. Yao (2004) PNAS 101, 7851-7856

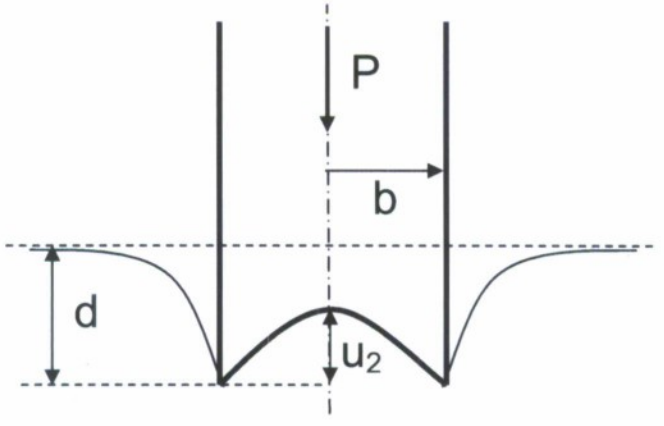

Figure 10. Illustration of a rigid cylindrical punch, indenting an elastic half space. The punch is a spherically concave at its bottom and the depth of the concavity is u_2. d is the depth of indentation, b is the radius of punch and P is the applied force. In the presence of adhesion, a negative force P is necessary to separate the two solids.

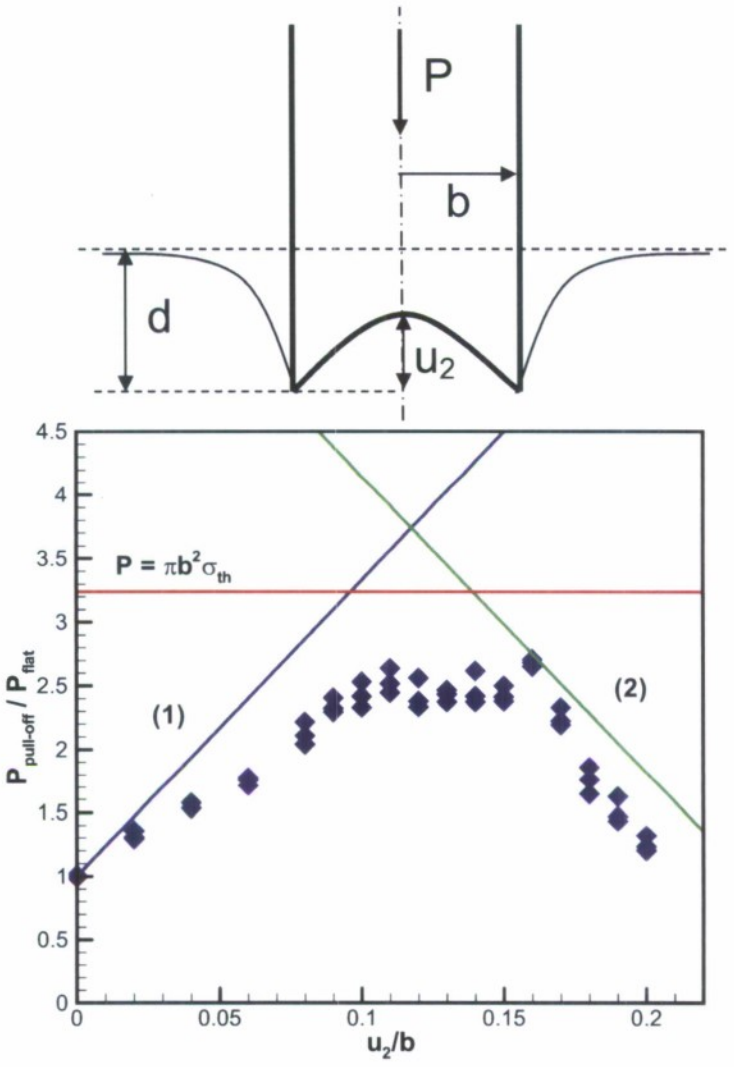

Fig. 11. The top figure shows the schematic illustration of a rigid concave punch indenting an elastic half space. The depth of concavity is u_2. In the plot shown, the theoretical prediction of the detachment force (pull-off force) as a function of the depth of the concavity is shown as solid lines. The discrete points show the experimental results, which show good agreement with the theoretical predictions.

6. Fabrication of microstructures for bio-mimetic adhesion

This section outlines the fabrication and adhesion testing of the first successful micro-scale bio-mimetic sample produced for the current research project. Although the ultimate aim of this project is to fabricate samples that will exhibit traits similar to the anisotropic adhesion behavior of gecko toes, the work presented herein consists of symmetric mushroom-like (in the sense that they consist of a 'stem' and a flat 'top') samples that display isotropic adhesion properties; however, the methods used to fabricate the symmetric samples can be extended upon

to produce the desired asymmetric structures in the near future. As a starting point, the work performed hitherto serves as a solid foundation on which to explore this problem further.

Sample Fabrication

The basic idea behind fabricating micro-scale adhesion structures is to first create a sacrificial mould using micro-fabrication techniques, then to fill the mould with liquid PDMS under a vacuum and cure it until it is a solid, and finally to remove the mould, leaving nothing but the PDMS micro-structures behind. The first attempts at fabricating a mould utilized a silicon wafer as the mould material itself; the problem with this approach is that silicon etchants also violently attack PDMS, thus rendering the final samples heavily damaged and unusable for adhesion testing. In order to circumvent this problem, the mould material must be soluble in a substance that is harmless to PDMS. The answer, for the time being anyway, seems to be photoresist, which is easily soluble in acetone, a chemical that is innocuous towards PDMS.

The samples created for the work in discussion were moulded in photoresist that was processed using (almost) standard photolithography techniques in a clean-room. The first step in the process is to spin-coat a silicon wafer with Rohm-Haas SPR 220-7.0 positive photoresist at a thickness of approximately 5μm. The resist is then exposed to ultraviolet light without a mask in order to flood expose it and polymerize the entire layer; if the sample were to be placed in the developer solution after exposure, the entire layer would dissolve away in a matter of seconds. After the first exposure, the same type of photoresist is spun onto the first layer at a thickness of approximately 8μm. This second layer is then exposed through a mask, which consists of a pattern of a large array of 5μm squares - these squares form the 'stems' of the mushrooms. After the second exposure, the sample is placed in a hydroxide developer solution that begins to develop the exposed squares and creates extruded holes in the photoresist; once the holes (these holes form the 'stems') have been fully formed, the developer reaches the first exposed layer and begins to remove material in an isotropic fashion; this isotropic developing of the first layer is what creates the 'top' of the mushroom structure.

Upon completion of the developing, the mould is filled with liquid PDMS in a vacuum and cured at 75 degrees Celsius for 5 hours in order to solidify. After curing, the entire sample is placed in an acetone bath, which dissolves the photoresist mould and leaves the PDMS mushroom structures completely unscathed. The final PDMS structure is shown in Figure 12 at a magnification of 3000X; the mushroom 'tops' are approximately 12-13μm in diameter.